nature catalysis

Article

https://doi.org/10.1038/s41929-025-01357-y

A general photocatalytic platform for the regio- and stereoselective β-chloroacylation of alkenes and alkynes using a heteroleptic copper(I) complex

Received: 6 October 2024

Accepted: 9 May 2025

Published online: 24 June 2025

Check for updates

Tirtha Mandal [1,2], Mangish Ghosh [1,2], Hendrik Paps[1], Tanumoy Mandal[1] & Oliver Reiser [1]

Atom transfer radical addition (ATRA) of aroyl chlorides to access β-chloroacyl derivatives via photoredox catalysis remains hamstrung by the need to use precious iridium photocatalysts and activated alkenes as acceptors. Here we report a unified platform for the regioselective chlorocarbonylation of alkenes via visible-light-mediated ATRA of aroyl chlorides catalysed by a heteroleptic Cu(I) complex featuring extensive substrate scope, scalability and functional group tolerance. In addition, alkynes are amenable substrates, allowing *E*-selective β-chlorovinyl ketone formation. The synthetic utility of the protocol is demonstrated through the functionalization of complex substrates, post-modifications of the products and the formal synthesis of pharmacologically relevant haloperidol, seratrodast and the naturally occurring piperidine alkaloid (−)-sedamine. This study undergirds the exclusive role of a heteroleptic copper(I) complex, which outperforms homoleptic copper(I) complexes—efficient for many ATRA processes—owing to its longer excited-state lifetime and adaptive ligand environment being tailored for the distinctive mechanistic steps catalysed by Cu(I) and Cu(II) in the title reaction.

Atom transfer radical addition (ATRA) reactions, pioneered by Kharasch et al., increase molecular complexity through the selective difunctionalization of alkenes and alkynes with high atom and step economy[1,2]. When combined with visible-light photoredox catalysis[3], ATRA reactions can be markedly diversified[4]. Among the various photocatalysts that were discovered to promote ATRA processes, homoleptic copper(I)–phenanthroline complexes have enabled transformations, diverted conventional reaction pathways and fostered the invention of new catalytic modes given their ability to engage with substrates to act beyond single-electron transfer (SET) reagents[5–10]. The transformation can proceed either through a Cu(I)/Cu(II) catalytic cycle involving SET, ligand exchange and ligand transfer[11,12] or through a Cu(I)/Cu(II)/Cu(III) catalytic cycle involving SET-radical rebound, ligand exchange and reductive elimination[13,14] to ultimately deliver the products (Extended Data Fig. 1). A wide range of ATRA processes get accelerated due to the ability of Cu(II), a persistent radical, to intercept transient radical species generated via the addition of R• to an alkene or alkyne. Despite these remarkable advancements, organic molecules compatible with Cu(I)-photocatalysed ATRA processes are mainly limited to Csp^3–X precursors (X = halides, thiocyanates and so on)[15–19]. Cu(I)-promoted photoactivation of Csp^2–X molecules such as aroyl chlorides to perform ATRA of alkenes or alkynes to access β-chloroacyl derivatives represents an exciting frontier for future research and development.

[1]Institut für Organische Chemie, Universität Regensburg, Regensburg, Germany. [2]These authors contributed equally: Tirtha Mandal, Mangish Ghosh.
e-mail: oliver.reiser@chemie.uni-regensburg.de

https://doi.org/10.1038/s41929-025-01357-y

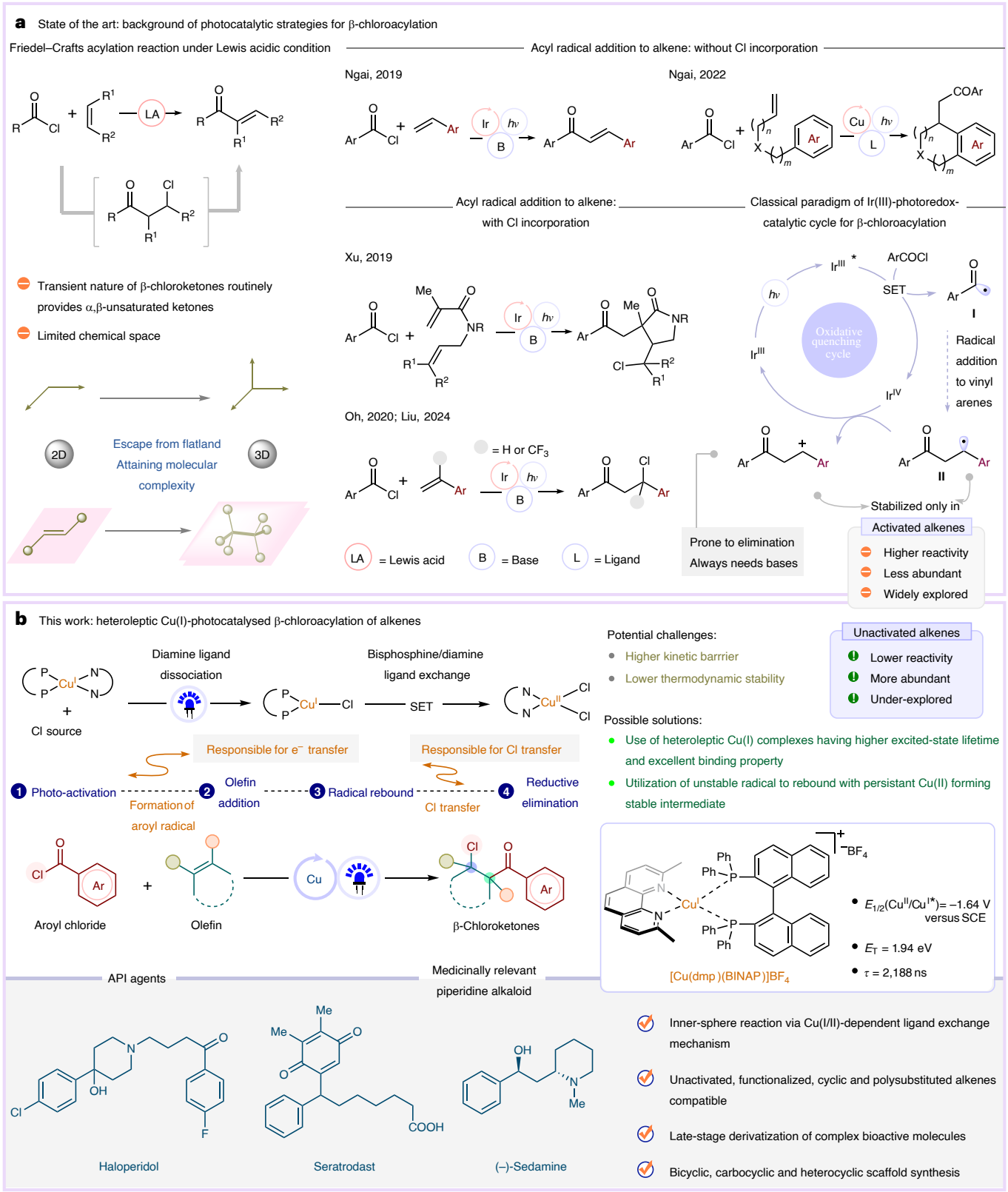

Fig. 1 | General overview of β-chloroacylation of alkenes. a, The state of the art in β-chloroacylation of alkenes (Ngai, 2019, 2022 (refs. 25,31), Xu, 2019 (ref. 33), Oh, 2020 (ref. 26) and Liu, 2024 (ref. 27)). * denotes the excited state of the photocatalyst. **b**, This work: photocatalytic β-chloroacylation of alkenes using a heteroleptic Cu(I) complex. E_T, triplet energy; τ, excited-state lifetime.

β-Chloroacylation of alkenes using the well-known Friedel–Crafts acylation generally leads to the formation of α,β-unsaturated ketones due to the instability of β-chloroketones under acidic conditions[20–22] (Fig. 1a). Thus, the thermal reaction modes to access β-chloroketones are limited to $BiCl_3$-catalysed chlorination of β-silyloxy ketones using trimethylsilyl chloride[23] and $SiCl_4$/PhOH-promoted hydrochlorination of α,β-unsaturated ketones[24]. In 2019, the Ngai group developed the proton-coupled electron-transfer-mediated chloroacylation of styrenes from aroyl chlorides (E^{red} = −1.26 V versus saturated calomel electrode (SCE) for benzoyl chloride) using *fac*-Ir(ppy)$_3$ ($E^{red}_{1/2}$*($*Ir^{3+}$/Ir^{4+}) = −1.73 V versus SCE) for the synthesis of α,β-unsaturated ketones in which 2,6-di-*tert*-butyl-4-methyl-pyridine was used to form the corresponding *Py-HCl as a proton-coupled electron-transfer catalyst[25] (Fig. 1a). While this work formally constitutes the photolytic Friedel–Crafts acylation of styrenes, the isolation of β-chloroketones was achieved only for two substrates after a reverse-phase high-performance liquid chromatography purification. Recently, the visible-light-mediated intermolecular β-chloroacylation of styrenes and α-CF_3-substituted styrenes has been reported separately by Oh et al.[26] and Liu et al.[27] using *fac*-Ir(ppy)$_3$ as the photocatalyst (Fig. 1a). Nevertheless, its translation to unactivated alkenes has proved elusive. The Xu group's and Ngai group's findings on the addition of acyl radical species to alkenes under photolytic conditions using Ir photocatalyst have led to the formation of fused pyran[28] and 3,3-dialkyl 2-oxindole derivatives[29] and functionalized 1,4-, 1,6- and 1,7-diketones[30] in an intramolecular fashion without chlorine incorporation. In addition, the photoactivation of aroyl chlorides using Cu(I)/*rac*-BINAP was reported by the Ngai group for the synthesis of different heterocycles and carbocycles via intramolecular radical cyclization following the addition of acyl radicals to alkenes with no chlorine incorporation[31,32] (Fig. 1a). By contrast, the Xu group reported aroylchlorination of 1,6-dienes via acyl radical addition to activated acrylamides followed by intramolecular atom transfer radical cyclization process using Ir(ppy)$_3$ as the photocatalyst (Fig. 1a)[33].

Despite the exceptional progress achieved, this type of transformation must be revised to avoid restrictions such as limited substrate scope and the use of precious Ir photocatalysts. The 1,2-chloroacylation of all kinds of alkene would produce molecules with greater three-dimensionality, thus offering a larger accessible chemical space that can be leveraged in pharmaceutical research. From previous reports, it can be concluded that the challenges associated with developing such a transformation are primarily due to the instability of the generated alkyl radical intermediate **II** unless it is benzylic (Fig. 1a, case of styrenes) or tertiary[33]. Further, using acid-sensitive Ir photocatalysts is hampered due to the necessity to use a base, resulting in the competitive elimination of the carbocation intermediate **III** (Fig. 1a). A Cu(I)-promoted photocatalytic ATRA platform has the potential to avoid the formation of cation **III** via an inner-sphere radical rebound mechanism initiated from a Cu(II)–Cl complex by chlorine atom transfer or by a radical capture generating a transient Cu(III) complex **IV** that forges the C–Cl bond through a reductive elimination (vide infra, Fig. 8a). However, such reactions have not been reported using the well-known Cu(I)–phenanthroline complexes despite having reduction potentials ($E_{Cu(II)/Cu(I)^*}$ = −1.43 V versus SCE for [Cu(dap)$_2$]Cl (dap, 2,9-di(*p*-anisyl)-1,10-phenanthroline) and $E_{Cu(II)/Cu(I)^*}$ = −1.54 V versus SCE for [Cu(dmp)$_2$]Cl) (dmp, 2,9-dimethyl-1,10-phenanthroline)[34] that are sufficient to reduce aroyl chlorides. This may be a consequence of the short excited-state lifetimes (90 ns to 270 ns) of homoleptic Cu(I)–phenanthroline complexes to execute the single electron reduction of aroyl chlorides. We posited heteroleptic Cu(I)–bisphosphine–phenanthroline complexes could emerge as a selective and sustainable alternative owing to their longer excited-state lifetimes and specialized dual ligand environment. Despite the introduction of such heteroleptic Cu(I) complexes in photochemistry three decades ago[35–37], their utility in organic synthesis has remained underexplored[37–48].

In this work, we identify [Cu(dmp)(BINAP)]BF_4 as an easy-to-prepare and bench stable Cu(I) complex (Fig. 1b) that establishes a unified platform for the β-chloroacylation of alkenes. Our study reveals that both the excited-state lifetime and ligand environment of the heteroleptic Cu(I) photocatalyst are crucial to the outcome of the reaction. A key aspect is the different coordination modes of the ligands to Cu(I) and Cu(II): while the sterically bulky bisphosphine ligand provides the environment for Cu(I) boasting of a sufficient excited-state lifetime and reduction potential to achieve the initial one-electron reduction of the acyl chlorides, the bisdiamine ligand exclusively coordinates to Cu(II), allowing the chloride transfer to the carbon-centred radicals generated as reactive intermediates (Fig. 1b). Thus, synthetically versatile β-chloroaroyl compounds become widely accessible from different classes of alkenes or alkynes, surpassing classical, photocatalysed acyl radical additions that are restricted to activated alkenes.

Results

Reaction development

We explored the possibility of a β-chloroacylation of alkenes using unactivated 1-phenylbutene (**A1**) and benzoyl chloride (**B1**) in the presence of catalytic amounts of various homo- and heteroleptic Cu(I) complexes under irradiation with a blue light-emitting diode (LED; Fig. 2; for more details, see Supplementary Tables 1–5). Several critical reaction parameters were recognized. Using tetrahydrofuran (THF) as the solvent at a concentration of 0.0625 M is best for the success of the reaction, which moreover takes an active role in the acyl radical coupling with electron-deficient alkenes (vide infra, see Fig. 8h). Using homoleptic Cu(I) complexes [Cu(dap)$_2$]Cl and [Cu(dmp)$_2$]Cl resulted in no product formation, probably due to their insufficient excited-state lifetimes. Moving to heteroleptic Cu(I) complexes, [Cu(dmp)(BINAP)]BF_4 (BINAP, 2,2′-bis(diphenylphosphino)-1,1′-binaphthyl) gave rise to the desired product **1** in 76% yield, while other Cu(I) heteroleptic complexes such as [Cu(dmp)(XantPhos)]BF_4 (XantPhos, (9,9-dimethyl-9*H*-xanthene-4,5-diyl)bis(diphenylphosphane)) and [Cu(phen)(XantPhos)]BF_4 (phen, 9,10-phenanthroline) were vastly inferior (7–12% yield), which is again in agreement with their much shorter excited-state lifetime values. The presence of base (Na_2CO_3) negatively impacted the efficiency of the reaction. Control experiments confirmed the necessity for light and the Cu(I) catalyst. Furthermore, an inert atmosphere is essential for this reaction; only trace amounts of product were generated when the reaction was performed in air. When styrene **A2**, as an example of an activated alkene, was used, the desired product **2** was obtained in near-quantitative yield under the standard reaction conditions, being superior to other variations tried (for detailed optimization, see Supplementary Table 6). The protocol developed here operates at room temperature and does not require base and additional oxidants or reductants.

Substrate scope evaluation

Having established the optimized conditions, we examined the substrate scope of this transformation (Fig. 3). Simple unfunctionalized aromatic and aliphatic alkenes could be smoothly converted to β-chloroketones in 59–80% yields (Fig. 3a, **1** and **3**–**6**). Various transformable handles, including halides (**7** and **8**), aldehyde (**9**), ketone (**10**), ester (**11**), cyano (**12**), acid (**13**) and amide (**14**) were well tolerated at different positions of the aliphatic chains. The limitation was found for amino or hydroxyl groups present in the alkene. Such substrates underwent direct coupling with the acid chloride used: **15** was not observed at all, while **17** was obtained only in low yield (25%). Instead, protected amine (NHBoc; Boc, *tert*-butyloxycarbonyl) and hydroxyl (OTBDMS, OTs; TBDMS, *tert*-butyldimethylsilyl) alkene derivatives proceed in good yields (**16**, **18** and **19**). Alkenes bearing heterocycles such as oxirane, carbazole and phenothiazine moieties were compatible with this transformation (**20**–**22**). Boron- and silicon-containing alkenes were also successful,

https://doi.org/10.1038/s41929-025-01357-y

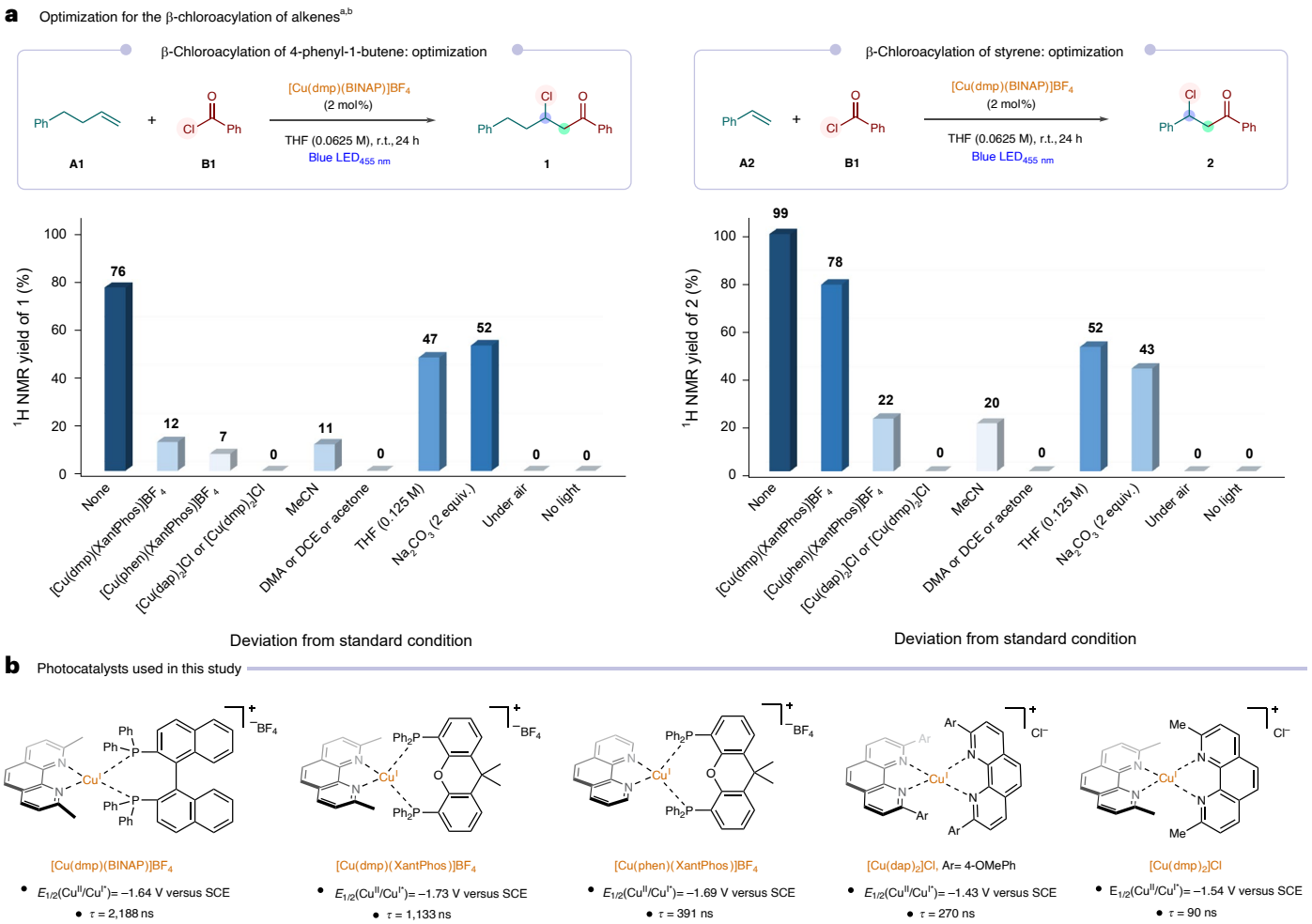

Fig. 2 | Optimization of the reaction conditions. a, Optimization for the β-chloroacylation of alkenes: Condition 1: **A1** (0.5 mmol), **B1** (0.25 mmol), [Cu(dmp)(BINAP)]BF_4 (2 mol%), THF (4 ml), blue LED, room temperature (r.t.), 24 h. Condition 2: **A2** (0.25 mmol), **B1** (0.5 mmol), [Cu(dmp)(BINAP)]BF_4 (2 mol %), THF (4 ml), blue LED, r.t., 24 h. [a]The bar diagram is prepared on the basis of a single experiment for each entry and corresponding NMR yield values. [b]The ^{1}H-NMR yields are measured using 1,1,2,2-tetrachloroethane as the internal standard. **b**, Photocatalysts used in this study. None, standard reaction conditions; DCE, dichloroethane; DMA, dimethylacetamide.

forming the difunctionalized products **23** and **24**. Di- and trisubstituted alkenes smoothly afforded the desired products **25** and **26**; however, no conversion was observed for tetrasubstituted alkenes. Six- to eight-membered cyclic alkenes with internal double bonds proved to be efficient substrates (**27**–**29**) with moderate-to-excellent diastereoselectivity. The high site selectivity for β-chloroacyl derivatives **26** and **29** may arise from the synergistic steric and stereoelectronic effects upon radical addition. Moreover, exocyclic alkenes exhibited perfect regio- and stereoselectivity to provide **30** and **31**. The X-ray crystal structure of **30** confirms the configuration of the major diastereomer (Supplementary Fig. 32). To demonstrate the preparative utility, β-chloroketones **1** and **30** were synthesized on a 5.0 mmol scale without a substantial decrease in yield (70% and 58%, respectively; Fig. 3a).

Moving away from unactivated alkenes, the protocol was then applied to a variety of functionalized styrenes (Fig. 3b). A selection of vinyl arenes decorated with both electron-donating and electron-withdrawing substituents afforded the desired difunctionalized products (**2** (see Supplementary Fig. 31 for X-ray analysis of compound **2**), **32**–**37** and **40**–**52**) in generally high yields (>70%) with no apparent preference for the electronic nature of the aryl substituent. Notably, highly electron-deficient pentafluoro styrene, also in combination with steric congestion as seen for 2,6-dichlorostyrene, furnished the products **43** and **45**. Functional groups such as benzyl chloride (**49**), trimethylsilyl (TMS) (**50**), carboxylic acid (**51**) and boronic acid (**52**) were also well tolerated. Substituents flanking the α- or β-position of the styrene gave the desired products **53** and **54**. Of note, β-chloroacylation of indene selectively provided the *trans*-isomer **56**. β-Chloroacylation of vinyl naphthalene provided compound **57**; however, vinyl pyridines showed no conversion, perhaps due to its coordination with higher-valence copper ion (for example, **58** could not be obtained). In the case of styrene derivatives bearing *para*-methoxy and α-phenyl groups, the corresponding dehydrochlorinated products (**38**, **39** and **55**) were formed, which might be an indication for a change in mechanism, that is, that for these substrates the oxidation of the radical intermediate of type **II** (Fig. 1b) to the cation **III** proceeds as opposed to delivering the chlorine via an intermediate **IV** (cf. Fig. 8a).

Next, we examined a series of aroyl chlorides using 1-octene or styrene as the alkene component (Fig. 3c, **59**–**68**), in which the substituents on the aromatic ring exhibited neither a pronounced steric or electronic effect on the efficiency. The structure of thiophene **68** was unambiguously confirmed by single-crystal X-ray analysis (Supplementary Fig. 33).

Late-stage modification

The robustness and high site selectivity showcased suggest that it can be used as a precision tool to perform late-stage modifications of

https://doi.org/10.1038/s41929-025-01357-y

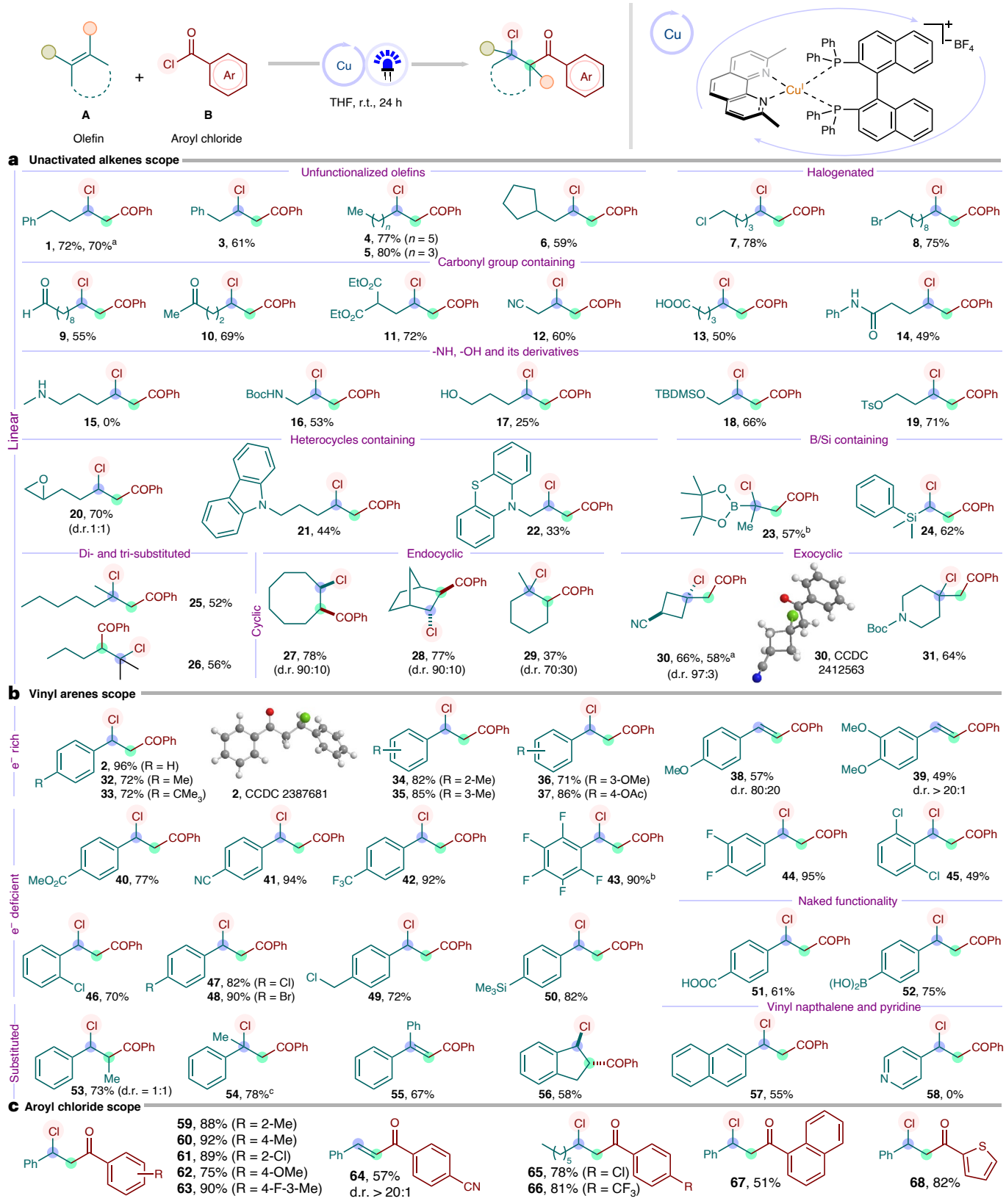

Fig. 3 | Substrate scope of alkenes. a, The scope of unactivated alkenes. **b**, The scope of vinyl arenes. **c**, The scope of aroyl chloride. Condition 1 (for unactivated alkenes): **A** (0.5 mmol), **B** (0.25 mmol), [Cu(dmp)(BINAP)]BF_4 (2 mol%), THF (4 ml), blue LED, r.t., 24 h. Condition 2 (for activated alkenes): **A** (0.25 mmol), **B** (0.5 mmol), [Cu(dmp)(BINAP)]BF_4 (2 mol%), THF (4 ml), blue LED, r.t., 24 h. [a]Reaction performed on a 5.0 mmol scale. [b]Compounds are obtained as a mixture of ATRA and dehydrochlorination products due to rapid HCl elimination during column chromatography. [c]Crude yield of the product is mentioned with respect to NMR internal standard as the product is column unstable. Unless otherwise noted, yields are calculated on the basis of the isolated products. d.r., diastereomeric ratio.

https://doi.org/10.1038/s41929-025-01357-y

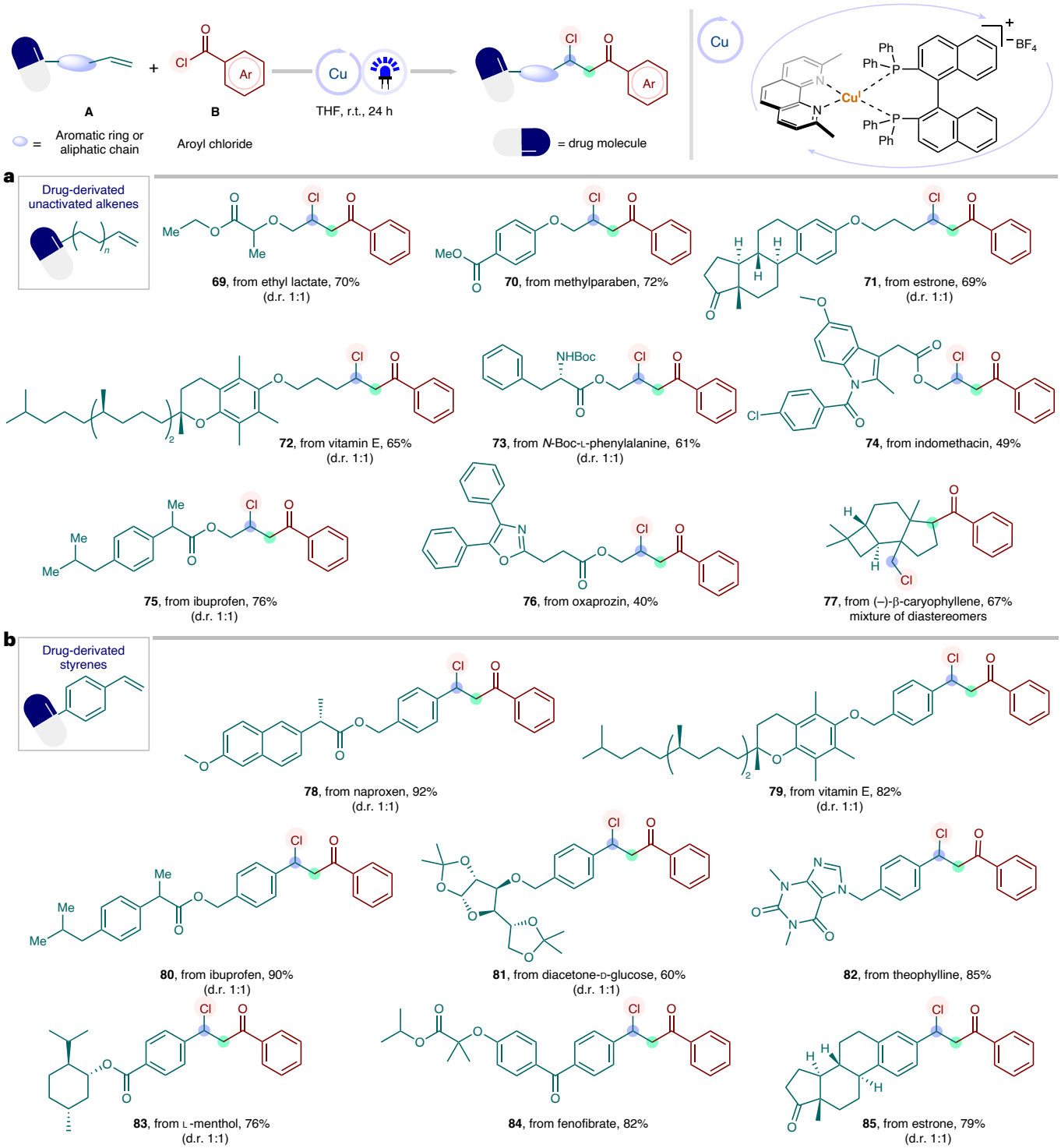

Fig. 4 | Late-stage functionalization of alkenes. a, β-Chloroacylation of unactivated alkenes derived from natural products and pharmaceuticals. **b**, β-Chloroacylation of vinyl arenes derived from natural products and pharmaceuticals. Condition 1 (for unactivated alkenes): **A** (0.3 mmol), **B** (0.25 mmol), [Cu(dmp)(BINAP)]BF_4 (2 mol%), THF (4 ml), blue LED, r.t., 24 h. Condition 2 (for activated alkenes): **A** (0.25 mmol), **B** (0.5 mmol), [Cu(dmp)(BINAP)]BF_4 (2 mol%), THF (4 ml), blue LED, r.t., 24 h. Yields are calculated on the basis of the isolated products. d.r., diastereomeric ratio.

biologically relevant scaffolds (Fig. 4). Unactivated alkenes derived from ethyl lactate, methyl paraben, estrone, vitamin E, phenyl alanine, indomethacine, ibuprofen and oxaprozin were converted into the corresponding β-chloroketones **69**–**76** (Fig. 4a). In (−)-β-caryophyllene, featuring both endocyclic and exocyclic double bonds, the acyl radical addition took place selectively at the endocyclic one, affording **77** as a mixture of diastereomers.

Furthermore, a variety of vinyl arenes derived from natural products and pharmaceutical agents were compatible, demonstrating a viable approach for their modification (Fig. 4b, **78**–**85**).

β-Chloroacylation of alkynes

Next, we extended this methodology to the β-chloroacylation of alkynes. The well-known Friedel–Crafts acylation of alkynes with acid

https://doi.org/10.1038/s41929-025-01357-y

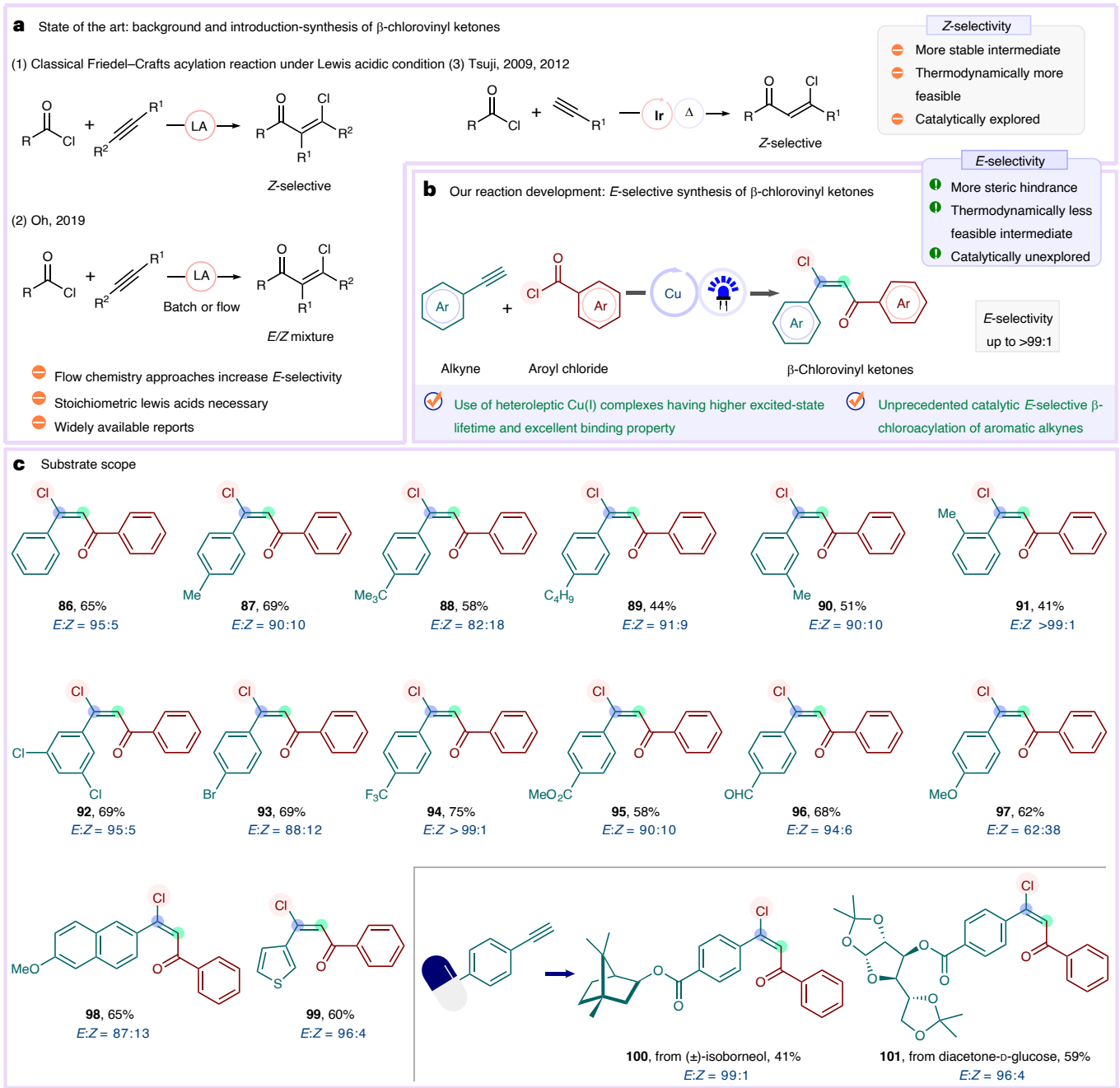

Fig. 5 | General overview of Cu(I)-photocatalysed β-chloroacylation of alkynes. a, The state of the art in β-chloroacylation of alkynes (Tsuji, 2009, 2012 (refs. 51,52); Oh, 2019 (ref. 53). **b**, This work: photocatalytic *E*-selective β-chloroacylation of alkynes using a heteroleptic Cu(I) complex. **c**, Substrate scope. Reaction conditions: aromatic alkyne (0.5 mmol), aroyl chloride (0.25 mmol), THF (4 ml), [Cu(dmp)(BINAP)]BF_4 (2 mol%), blue LED, r.t., 24 h. Yields are calculated on the basis of the isolated products. LA, Lewis acid.

chlorides[49,50] and Ir-catalysed addition of acid chlorides to alkynes[51,52] to access β-chlorovinyl ketones generally proceeds with complete *Z*-selectivity (Fig. 5a). Recently, the Oh group has developed the Friedel–Crafts acylation of alkynes in a flow set-up to increase the *E*-selectivity in β-chlorovinyl ketone formation[53] (Fig. 5a). However, the *E*-selective β-chloroacylation of alkynes in a catalytic manifold has not been reported.

Upon combining phenylacetylene **A3** with benzoyl chloride **B1** in the presence of 2 mol% [Cu(dmp)(BINAP)]BF_4 under blue-light irradiation, the β-chlorovinyl ketone **86** was obtained as a single regioisomer in 65% yield with excellent *E*-stereoselectivity (*E*:*Z* = 95:5; Supplementary Table 7). Likewise, *para*- and *meta*-alkyl substituted phenylacetylenes were suitable substrates (Fig. 5c, **87**–**90**). The reaction yield was hampered by *ortho* substitution on the aryl motif (**91**) with increased steric hindrance; however, it did not affect the stereoselectivity. Functional groups, such as halides (**92** and **93**), trifluoromethyl (**94**), ester (**95**) and aldehyde (**96**) were tolerated well in terms of both yield and *E*-selectivity. In the case of electron-rich arene alkynes, β-chlorovinyl ketones **97** and **98** were obtained in good yields but with notably decreased *E*-selectivity. However, 3-thiophenylacetylene afforded the corresponding β-chlorovinyl ketone **98** with excellent *E*-selectivity. Phenylacetylenes derived from (±)-isoborneol and diacetone D-glucose furnished **100** and **101**, again with almost perfect *E*-selectivity (Fig. 5c). However, disubstituted alkynes such as

1-phenyl-1-propyne and unactivated alkynes such as 1-hexyne were found to be unreactive.

Synthetic utility

The synthetic value of β-chloroketones derived from vinyl arenes and phenylacetylenes is well documented in the literature[26,52] (Fig. 6a). Selecting some representative examples, such transformations can also be carried out efficiently, starting from **1** and **4** to obtain dihydropyrazole **102** and β-chloro alcohol **103** (Fig. 6b). In addition, we envisioned that the library of β-chloroketones available in our arsenal could be used further as pluripotent intermediates for skeletal diversification (Fig. 6b). NaH-mediated dehydrochlorination of **103** provided exclusively homoallylic alcohol **104** as a single diastereomer. Taking advantage of this synthetic pathway, alkene diol **106** was synthesized starting from **8** in 77% yield, which was transformed to the linear hydrocarbon phenyldodecane (**107**) after mesyl protection and hydrogenation. The reduction–elimination sequence of cyclic β-chloroketone **30** led to the formation of oxabicyclo[3.2.0]heptane derivative **108** possibly via intramolecular Michael addition of intermediate **VII**. Moreover, we demonstrated that this strategy could be utilized in the construction of pyrrolodinone **109** in 88% yield by NaH-mediated cyclization of **14**. 2-Phenyltoluene (**110**) was efficiently synthesized via an intramolecular McMurry coupling–dehydrochlorination–aromatization cascade of chloroketone **10**. Furthermore, 3-chloropropiophenone **111**, a key synthetic intermediate to access (*R*)/(*S*)-fluxeotine, tomoxetine and nisoxetine[54], could be obtained by exposing **24** to potassium *tert*-butoxide in dimethyl sulfoxide (DMSO; Fig. 6c). Epoxy-alcohol **112** was received by a desilylative cyclization followed by conversion to 1,3-diol **113** using reported methods[55,56], being valuable for the synthesis of fesoteridone[57], dapoxetine[58], atomoxetine[59] and ezetimibe[60] (Fig. 6c).

Formal synthesis of haloperidol, (±)-seratrodast and (−)-sedamine

The potential of this method was further underpinned by the formal synthesis of active pharmaceutical ingredients haloperidol, seratrodast and naturally occurring piperidine alkaloid (−)-sedamine. Haloperidol is extensively used in the treatment of schizophrenia and Tourette's syndrome. The first synthesis of ^{18}F-labelled haloperidol was accomplished in a multistep process starting from *N*-phenylacetamide **114** and 4-chlorobutanoyl chloride **115** followed by nucleophilic displacement with commercially available piperidine nucleophile **116** (ref. 61). Recently, the MacMillan group elegantly reported a photoredox-enabled aldehyde C–H alkylation strategy for the synthesis of γ-chloroarylketone **120** via coupling of 4-chlorobutanal **119** and 1-bromo-4-fluorobenzene **118** (ref. 62). Nucleophilic displacement of ketone **120** with piperidine **116** delivered haloperidol **117**. However, the practical usefulness of this approach is hampered by the use of very expensive 4-chlorobutanal[63]. By adding commercially available and inexpensive 4-fluorobenzoyl chloride **B2** and allyl chloride **A4** to our reaction conditions followed by one-pot elimination and subsequent chemoselective double-bond reduction, the desired ketone **120** was afforded in 61% yield over two steps, which can be converted to haloperidol **117** following reported methods[62] (Fig. 7a). Moreover, γ-chloroarylketone **120** can be used to obtain dehydroxyhaloperidol, melperone, lenperone and fluanisone via nucleophilic displacement with commercially available corresponding piperidine derivatives. The synthesis of seratrodast, an antiasthmatic and eicosanoid antagonist, was reported by Takai and co-workers[64]. The key intermediate **122** was prepared via In-catalysed reaction of diketone **121** with ethanol (EtOH) followed by $NaBH_4$ reduction. In our approach, β-chloroacylation of methyl-5-hexenoate **A5** with benzoyl chloride **B1** furnished the compound **125**. Base-mediated dehydrochlorination and subsequent reduction delivered the desired alcohol ester derivative **126**, which can be transformed to seratrodast using a literature method[64] (Fig. 7b). Sedamine, a piperidne alkaloid, first isolated from *Sedum acre*[65], has been synthesized either as a racemate[66–70] or as a single enantiomer[71–80]. The first synthesis of (−)-sedamine **132** was documented by the Beyerman group in 1956. Metal-hydride-mediated sequential reduction of aminoalcohol **129** and ketoacid **130** led to the formation of racemic sedamine **131**, which could be converted to (−)-sedamine **132** by optical resolution[71,72] (Fig. 7c). Ag-catalysed asymmetric Mannich reaction was developed by the Hoveyda group for the synthesis of (−)-sedamine using chiral ligand **136** (ref. 76). Our method facilitates the generation of the piperidinone building block **139** (refs. 68,72) of (−)-sedamine directly from amide **A6** and benzoyl chloride **B1** in two steps with 54% overall yield, allowing a greatly streamlined β-chloroacylation–cyclization sequence (Fig. 7c). Importantly, this approach underscores the potential for the rapid library synthesis of different lactam analogues (for example, **109**; cf. Fig. 6).

Mechanistic investigation and proposed catalytic cycle

The developed method can be performed chemoselectively on activated alkenes over unactivated ones, as illustrated by the preferential formation of mono-chloroacylated product **140** (Extended Data Fig. 2a). When 3 equiv. of benzoyl chloride **B1** were used, the di-chloroacylated product **141** was formed exclusively. Alternatively, the di-chloroacylated product **141** can be obtained by sequential reaction at the activated and unactivated double bonds (Extended Data Fig. 2a). The reaction of diene **A8** proceeds in a 1,4-fashion delivering the product **142** with excellent diastereoselectivity (Extended Data Fig. 2b). A radical trap experiment performed by adding 2,2,6,6-tetramethyl-1-piperidinyloxy (TEMPO), completely inhibited the reaction and produced the aroyl-TEMPO adduct **144** (Extended Data Fig. 2d), supporting the formation of an aroyl radical. In agreement, using the radical clock reagent β-pinene **A9** under the standard conditions provided exclusively **143** through the aroyl radical initiated ring-opening followed by chlorine incorporation (Extended Data Fig. 2c). The quantum yield of the standard reaction was measured to be 0.046, which indicates that an extended radical chain process is unlikely (Supplementary Table 8). Ultraviolet–visible (UV–vis) absorption shifts of the binary mixture of photocatalyst [Cu(dmp)(BINAP)]BF_4 and benzoyl chloride **B1** before irradiation indicated coordination of ATRA reagent **B1** to the photocatalyst (Extended Data Fig. 2e and Supplementary Figs. 6 and 7). Stern–Volmer quenching experiments revealed that aroyl chloride **B1** quenched the excited [Cu(dmp)(BINAP)]BF_4 species more efficiently than the alkene substrate **A1** (Extended Data Fig. 2f and Supplementary Fig. 10). Next, we analysed the impact of excited-state lifetime and ligand environment of heteroleptic Cu(I) photocatalysts. Besides the three heteroleptic Cu(I) photocatalysts that were screened during optimization (cf. Fig. 2), we additionally evaluated [Cu(phen)(BINAP)]BF_4 (τ = 3 ns) and [Cu(dmp)(DPEPhos)]BF_4 (τ = 14,300 ns) (DPEPhos, bis[(2-diphenylphosphino)phenyl]ether) with contrasting excited-state lifetime values to compare their efficacy (Extended Data Fig. 2g). The reduction potential of the catalysts is capable of reducing aroyl choride **B1**, but nevertheless gave different outcomes. The highest yield of **1** was obtained using [Cu(dmp)(BINAP)]BF_4 having τ = 2,188 ns. Intriguingly, when [Cu(dmp)(DPEPhos)]BF_4 is used, the desired β-chloroketone **1** was obtained in 10% yield despite having a very high excited-state lifetime of 14,300 ns. A similar trend was observed for [Cu(dmp)(XantPhos)]BF_4 (τ = 1,133 ns). These results suggested that the presence of BINAP as a bidentate phosphorous ligand is crucial as the narrower bite angle of BINAP compared with DPEPhos and XantPhos renders [Cu(dmp)(BINAP)]BF_4 less photostability[48], facilitating faster dissociation of the dmp ligand (cf. Fig. 8). However, [Cu(phen)(BINAP)]BF_4 with an excited-state lifetime of only 3 ns provided the β-chloroketone **1** in 30% yield, highlighting the importance of substituted diamine ligand (dmp) compared with unsubstituted one (phen) providing a longer excited-state lifetime to the Cu(I) catalysts[48]. These results underscore the importance of a specialized ligand environment of heteroleptic Cu(I) photocatalysts comprising both bidentate phenanthroline and

https://doi.org/10.1038/s41929-025-01357-y

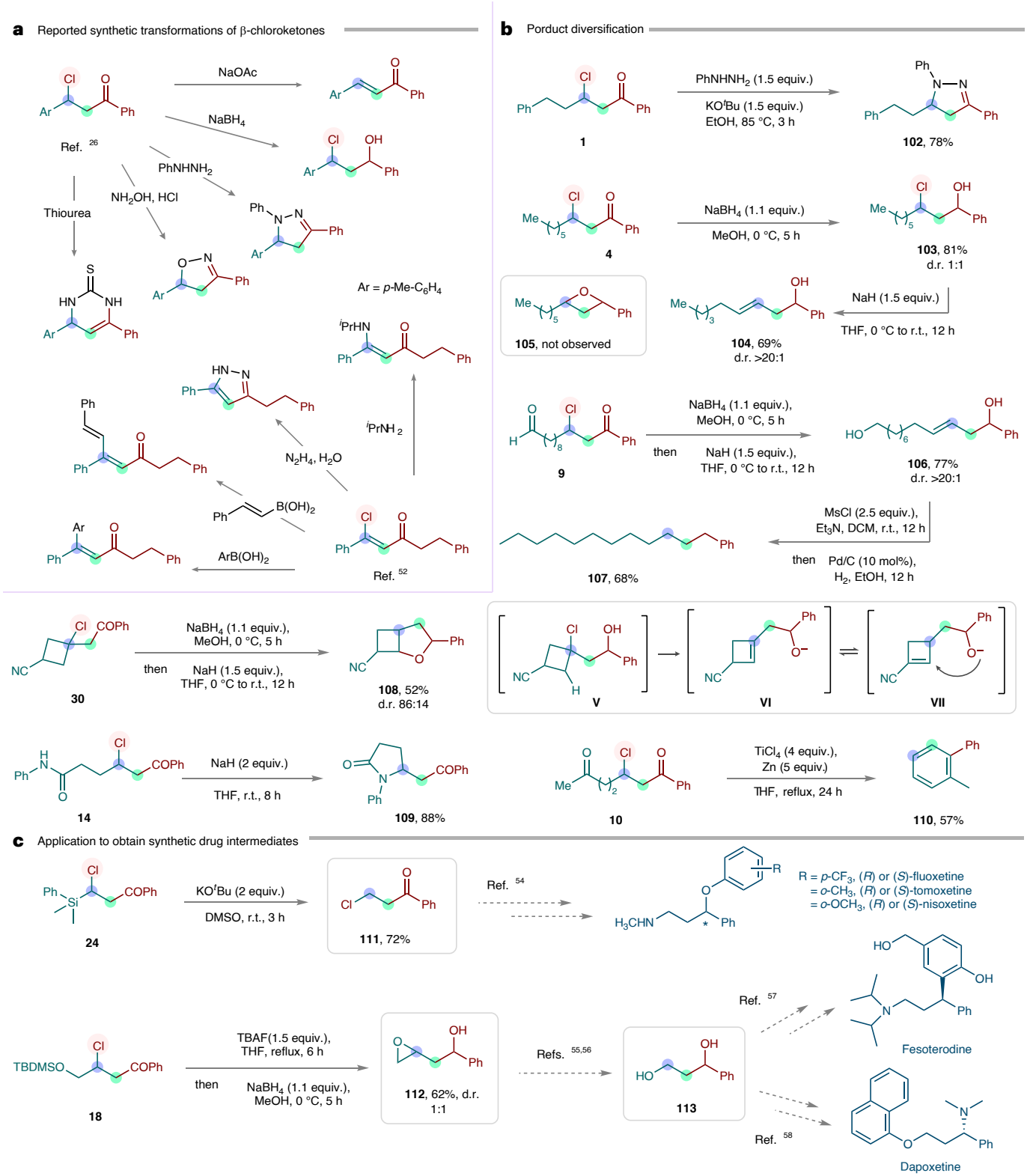

Fig. 6 | Synthetic applications. a, Reported synthetic transformations of β-chloroketones. **b**, Product diversification. **c**, Application to obtain synthetic drug intermediates. All the reactions are carried out in 0.2 mmol scale. Yields are calculated on the basis of the isolated products. * in **c** denotes the presence of a stereocentre at the C atom. DCM, dichloromethane; TBAF, tetrabutylammonium fluoride.

phosphine ligands in its coordination sphere for obtaining the highest catalytic efficiency in the title reaction. Moreover, to assess the efficiency of the formation of Cu(III)-species of type **IV** we conducted the ATRA of alkene **A10** where β-chloroacylation competes with intramolecular cyclization (Extended Data Fig. 2h). In 2022, Ngai et al. reported that reaction of alkene **A10** with aroyl chloride led to the formation of heterocycle **146** via an intramolecular cyclization-aromatization pathway[31]. Conversely, under the standard reaction conditions developed in this work, ATRA product **145** was obtained exclusively in 62% yield, pointing towards a different course of the reaction pathway. In Ngai's work, the combination of $[Cu(BINAP)_2]PF_6$ and $[Cu(IPr)_2]PF_6$ as the catalytically active species was postulated, where the homoleptic

https://doi.org/10.1038/s41929-025-01357-y

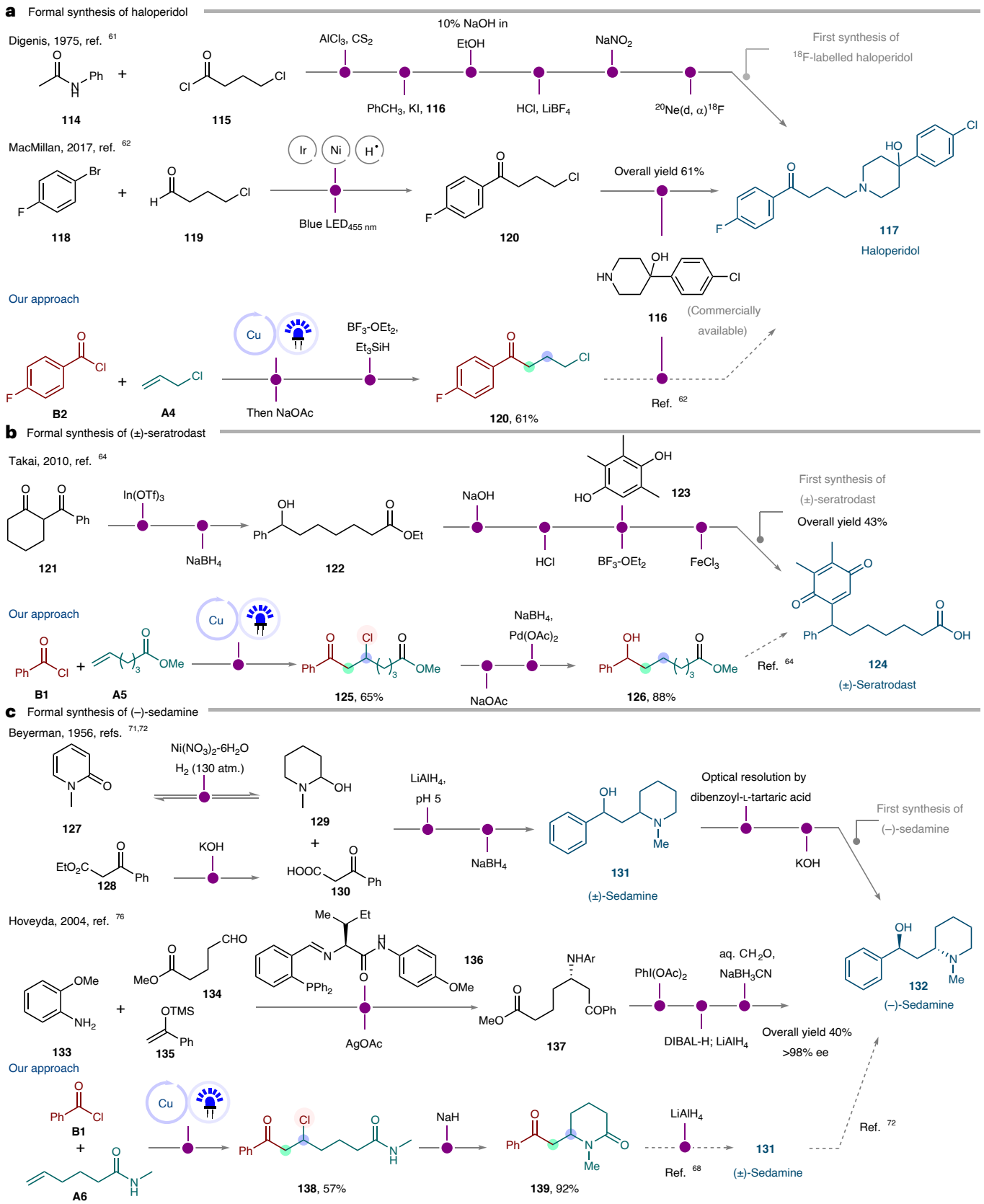

Fig. 7 | Formal synthesis of pharmaceuticals and bioactive molecules. a, Formal synthesis of haloperidol. **b**, Formal synthesis of (±)-seratrodast. **c**, Formal synthesis of (−)-sedamine. OTMS, *O*-trimethylsilyl; aq. aqueous; ee, enantiomeric excess.

https://doi.org/10.1038/s41929-025-01357-y

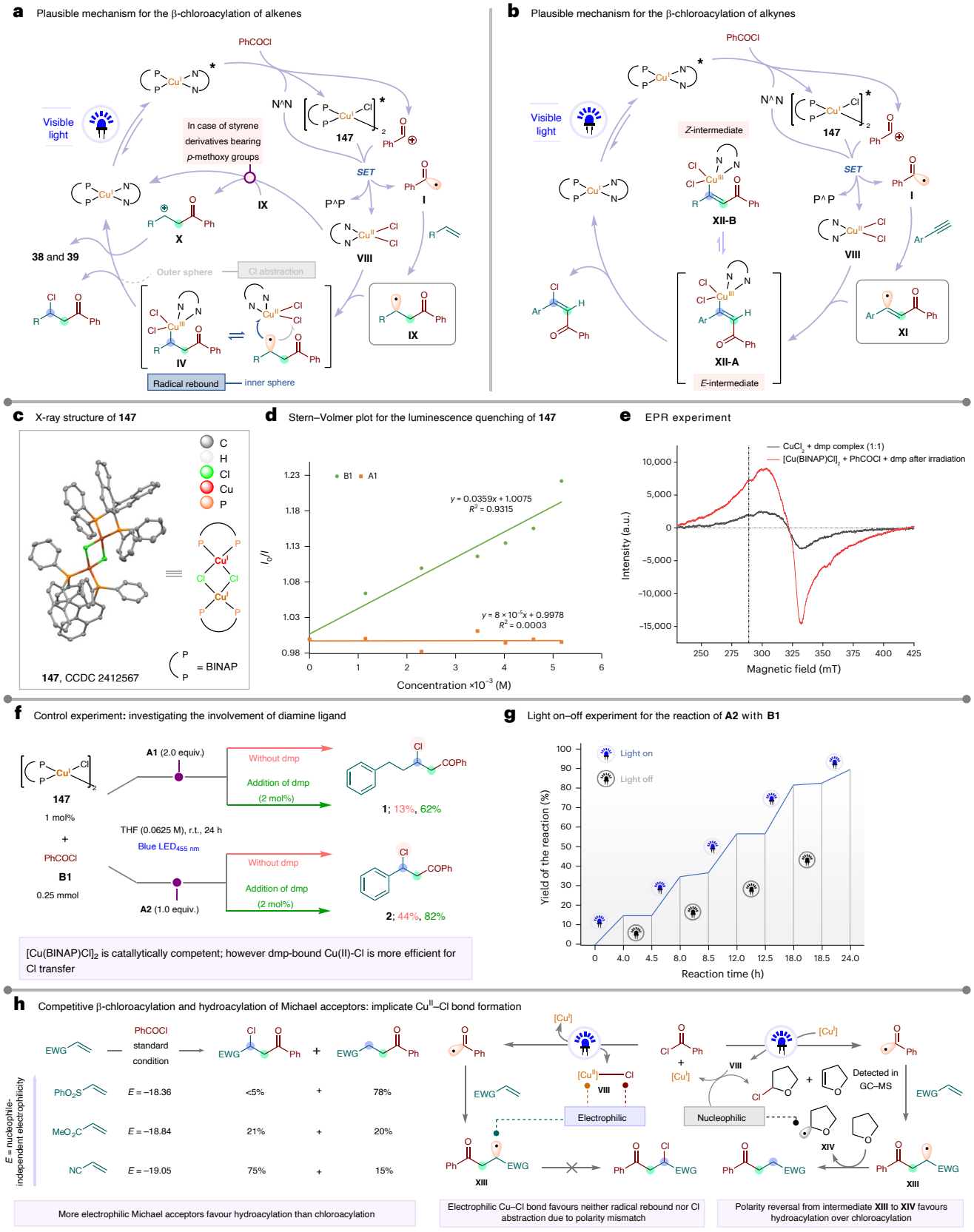

Fig. 8 | Proposed catalytic cycle and detection of Cu(I)/Cu(II) intermediates. **a**, The proposed catalytic cycle for the β-chloroacylation of alkenes. **b**, The proposed catalytic cycle for the β-chloroacylation of alkynes. * in **a** and **b** denotes the excited state of the photocatalyst. **c**, The X-ray crystal structure of the Cu(I)–Cl complex **147**. **d**, A Stern–Volmer plot for luminescence quenching of Cu(I) catalyst **147** in the presence of aroyl chloride and alkene. I_0 is the rate of fluorescence, without a quencher; I is the rate of fluorescence in the presence of a quencher. **e**, An EPR experiment to detect the formation of dmp-bound Cu(II)–Cl intermediate **VIII**. **f**, Investigating the involvement of diamine ligand for Cl transfer. **g**, Light on–off experiment for the reaction of **A2** with **B1**. **h**, β-Chloroacylation versus hydroacylation of Michael acceptors: synthetic evidence for Cu(II)–Cl bond formation. GC–MS, gas chromatography–mass spectrometry. EWG, electron-withdrawing group.

$[Cu(BINAP)_2]PF_6$ is responsible for the reduction of aroyl chlorides[31]. We reason that the heteroleptic $[Cu(dmp)(BINAP)]BF_4$ performs a dual role via ligand exchange: reduction of aroyl chlorides and rapid capture of transient radical of type **IX** by persistent Cu(II)–Cl intermediate **VIII** to prevent competitive cyclization (cf. Fig. 8).

Investigating $[Cu(dmp)(BINAP)]BF_4$ in the presence of aroyl chloride, in the dark no ligand exchange is observed, while irradiation at 455 nm results in the rapid formation of the phosphine-bound bridged[81] Cu(I)–Cl complex **147** due to facile dissociation of the phenanthroline ligand (Fig. 8a). Cu(I)–Cl complex **147** was fully characterized by independent single-crystal X-ray analysis (Fig. 8c and Supplementary Fig. 34) and nuclear magnetic resonance (NMR) spectroscopy (Supplementary Figs. 16–18). The excited-state reduction potential of **147** ($E_{Cu(II)/Cu(I)^*}$ = −2.19 versus Fc^+/Fc; −1.81 V versus SCE; Supplementary Figs. 23 and 24) is sufficient to reduce benzoyl chloride as confirmed by Stern–Volmer analysis (Fig. 8d and Supplementary Figs. 19–21). Similar interaction between **147** and benzoyl chloride was observed in UV–vis spectra. Furthermore, a bathochromic shift in the UV–vis absorption spectra of complex **147** compared with $[Cu(dmp)(BINAP)]BF_4$ (Supplementary Fig. 22) can explain why the highest reaction efficiency was obtained when the reaction was performed above 400 nm, but not at 385 nm (Supplementary Table 5). Hence, **147** acts as the active photocatalyst to facilitate the formation of aroyl radical **I** upon one-electron reduction of benzoyl chloride or the corresponding benzoyl cation with the generation of phenanthroline Cu(II)–Cl species[34] **VIII** after a ligand exchange. The formation of Cu(II)–Cl species **VIII** was confirmed with the aid of electron paramagnetic resonance (EPR) and UV–vis spectroscopic studies (Fig. 8e, Supplementary Figs. 25–27 and Supplementary Table 9). The ligand exchange between BINAP and dmp is consistent with the change of oxidation state from Cu(I) to Cu(II), with the latter preferring the harder phenanthroline ligand to the softer bisphosphine ligand. This phenomenon in relation to Cu(I)/Cu(II) catalysis has previously been recognized by the Fu group for asymmetric amidation reactions[82]. The radical **I** adds to the alkene, forming the transient radical **IX**, which can interact with **VIII**. Chlorine is then transferred via an inner-sphere radical rebound mechanism initiated by a radical capture generating transient Cu(III) complex[18,19,83–85] **IV** that forges the C–Cl bond in the final product through a reductive elimination. Alternatively, direct chlorine abstraction from Cu(II)–Cl species **VIII** by radical **IX** may deliver the desired product in an outer-sphere pathway (Supplementary Figs. 12 and 13). The dual nature of the heteroleptic copper complex (Cu(I)–BINAP for SET and Cu(II)–dmp for chloride transfer) is further corroborated by the fact that neither $Cu(I)(dmp)_2Cl$ (cf. Fig. 2) nor $[Cu(I)\text{-}BINAP\text{-}Cl]_2$ **147** is capable to promote the title reaction efficiently, while independently prepared **147** to which dmp is added again results in good catalytic turnover (Fig. 8f). A light-on–off experiment (Fig. 8g and Supplementary Fig. 11) further suggests that the catalytic Cu(I) species responsible for SET can be reactivated upon light irradiation. For styrene derivatives bearing a strongly electron-donating *para*-methoxy group or an α-phenyl substituent, the reaction proceeds via a back-electron transfer mechanism by oxidation of the radical intermediate **IX** to the corresponding carbocation **X** followed by combination with the chlorine anion to **38**, **39** and **55** under regeneration of the photocatalyst. In case of aromatic alkynes, the vinyl radical intermediate **XI**, generated after aroyl radical **I** addition to alkynes, could interact with Cu(II)–chlorine intermediate **VIII**, leading to the formation of Cu(III) species **XII-A** or **XII-B** (Fig. 8b). Formation of the Cu(III) species presumably controls the stereoselectivity, and it is proposed that the reaction proceeds via the sterically more favoured intermediate **XII-A** to deliver the *E*-β-chlorovinyl ketone selectively upon reductive elimination. Previously, Collins et al. have reported that heteroleptic copper complexes can facilitate $E \leftrightarrow Z$ alkene isomerization under light irradiation via an energy transfer process due to their higher triplet energy and longer excited-state lifetime[86]. Accordingly, it would also be possible that chlorine abstraction from the Cu(II) species **VIII** by vinyl radical intermediate **XI** and ensuing photoisomerization in the presence of $[Cu(dmp)(BINAP)]BF_4$ leads to *E*-selective formation of β-chlorovinyl ketones (Supplementary Figs. 14 and 15). Further evidence for the Cu(II)–Cl species **VIII** as the chlorine atom transfer species was found for the β-chloroacylation of α,β-unsaturated Michael systems (Fig. 8h and Supplementary Fig. 28). With increasing electrophilicity of alkenes[87], the electrophilic alkyl radical **XIII** could neither bind with the electrophilic Cu(II) centre (inner-sphere pathway) nor it could abstract an electrophilic Cl atom from **VIII** (outer-sphere pathway). Instead, **XIII** abstracts a hydrogen atom from THF, resulting in the hydroacylation of the alkene (Fig. 8h). The nucleophilic THF-radical **XIV** then captures the Cl atom from **VIII**, aligned with the formation of 2-chlorotetrahydrofuran and dihydrofuran confirmed by gas chromatography–mass spectrometry analysis (Supplementary Figs. 29 and 30). Finally, it is understood that the ultimate proof of the mechanistic proposal would be the isolation of a Cu(III) intermediate along the reaction pathway, which represents a formidable challenge[88–90] given the rapid reductive elimination that can take place to yield the ATRA product with concurrent regeneration of the Cu(I) photocatalyst.

Conclusions

In summary, we have developed a highly efficient method for the β-chloroacylation of readily available alkenes and alkynes with aroyl chlorides. This modular approach leverages a heteroleptic Cu(I) photocatalyst to control acyl radical generation and C–Cl bond formation. It demonstrates remarkable compatibility with diverse functional groups and encompasses a broad substrate scope, thereby empowering the synthesis of valuable β-chloroketones across various chemical contexts, advocating this method to practical application in chemistry, pharmaceutical science and materials science. Notably, our design features the introduction of an *E*-selective β-chloroacylation of phenylacetylene derivatives in a catalytic manifold highlighting the efficient regio- and stereocontrol of this ATRA process for aromatic alkynes. The effectiveness of this protocol in late-stage contexts is demonstrated, allowing the rapid generation of molecular complexity from large and densely functionalized olefins derived from biomolecules and pharmaceuticals. The synthetic utility of this method is demonstrated via the construction of various heterocycle and carbocycle scaffolds and the preparation of molecules widely used as building blocks for the synthesis of different natural products. Furthermore, this method paves the way towards the formal synthesis of pharmaceutically relevant haloperidol and seratrodast and naturally occurring piperidine alkaloid (−)-sedamine, overcoming the limitation of the title reaction towards unactivated alkenes. Multifaceted mechanistic studies have revealed that the method exploits a heteroleptic copper complex in which a bidentate phosphine binds to Cu(I) to produce a photocatalyst to activate the aroyl chlorides, and a bidentate phenanthroline ligand binds to Cu(II) to effect highly efficient and expeditious rebound of Cu(II) after aroyl radical addition to olefins that can even outcompete a favourable intramolecular radical cyclization process[31].

Methods

$[Cu(dmp)(BINAP)]BF_4$-catalysed β-chloroacylation of unactivated alkenes using aroyl chlorides

To a glass reaction vial (5 ml size) equipped with a stir bar $[Cu(dmp)(BINAP)]BF_4$ (4.9 mg, 0.005 mmol), unactivated alkenes (if solid at room temperature, 0.5 mmol) and benzoyl chloride **B1** (30 µl, 0.25 mmol) were added. The vial was then sealed with a rubber septum and evacuated-backfilled with N_2 three times. Then, 4.3 ml of freshly distilled THF was added into the vial and the solution was purged with nitrogen for 7–10 min until a solution volume of around 4 ml. Then, unactivated alkene (if liquid at room temperature, 0.5 mmol) was added into the solution under positive nitrogen atmosphere. The vial was irradiated with blue LED (λ_{max} = 455 nm) at room temperature for

24 h. After completion of the reaction (monitored by thin layer chromatography (TLC) analysis), the whole reaction mixture was diluted with dichloromethane (DCM) and transferred to a round-bottom flask. Following concentration in vacuo, the crude product was purified by column chromatography on silica gel (eluent: hexanes and ethyl acetate in certain ratio as needed).

[Cu(dmp)(BINAP)]BF_4-catalysed β-chloroacylation of activated alkenes using aroyl chlorides

To a glass reaction vial (5 ml size) equipped with a stir bar [Cu(dmp)(BINAP)]BF_4 (4.9 mg, 0.005 mmol), activated alkenes (if solid at room temperature, 0.25 mmol) and benzoyl chloride **B1** (60 µl, 0.5 mmol) were added. The vial was then sealed with a rubber septum and evacuated-backfilled with N_2 three times. Then, 4.3 ml of freshly distilled THF was added into the vial and the solution was purged with nitrogen for 7–10 min until a solution volume of around 4 ml. Then, activated alkene (if liquid at room temperature, 0.25 mmol) was added into the solution under positive nitrogen atmosphere. The vial was irradiated with blue LED (λ_{max} = 455 nm) at room temperature for 24 h. After completion of the reaction (monitored by TLC analysis), the whole reaction mixture was diluted with DCM and transferred to a round-bottom flask. Following concentration in vacuo, the crude product was purified by column chromatography on silica gel (eluent: hexanes and ethyl acetate in certain ratio as needed).

[Cu(dmp)(BINAP)]BF_4-catalysed β-chloroacylation of aromatic alkynes using aroyl chlorides

To a glass reaction vial (5 ml size) equipped with a stir bar [Cu(dmp)(BINAP)]BF_4 (4.9 mg, 0.005 mmol), aromatic alkynes (if solid at room temperature, 0.5 mmol) and benzoyl chloride **B1** (30 µl, 0.25 mmol) were added. The vial was then sealed with a rubber septum and evacuated-backfilled with N_2 for three times. Then, 4.3 mL of freshly distilled THF was added into the vial and the solution was purged with nitrogen for 7–10 min until a solution volume of around 4 ml. Then, aromatic alkyne (if liquid at room temperature, 0.5 mmol) was added into the solution under positive nitrogen atmosphere. The vial was irradiated with blue LED (λ_{max} = 455 nm) at room temperature for 24 h. After completion of the reaction (monitored by TLC analysis), the whole reaction mixture was diluted with DCM and transferred to a round-bottom flask. Following concentration in vacuo, the crude product was purified by column chromatography on silica gel (eluent: hexanes and ethyl acetate in certain ratio as needed).

Data availability

The data supporting the findings of this study are available within the Article and its Supplementary Information and upon request from the corresponding author. Crystallographic data for the structures reported in this Article have been deposited at the Cambridge Crystallographic Data Centre, under deposition numbers CCDC 2387681 (**2**), 2412563 (**30**), 2387682 (**68**) and 2412567 (**147**). Copies of the data can be obtained free of charge at https://www.ccdc.cam.ac.uk/structures/. Source data are provided with this paper.

References

1. Kharasch, M. S., Jensen, E. V. & Urry, W. H. Addition of derivatives of chlorinated acetic acids to olefins. *J. Am. Chem. Soc.* **67**, 1626 (1945).
2. Kharasch, M. S., Jensen, E. V. & Urry, W. H. Addition of carbon tetrachloride and chloroform to olefins. *Science* **102**, 128 (1945).
3. Shaw, M. H., Twilton, J. & MacMillan, D. W. C. Photoredox catalysis in organic chemistry. *J. Org. Chem.* **81**, 6898–6926 (2016).
4. Courant, T. & Masson, G. Recent progress in visible-light photoredox-catalyzed intermolecular 1,2-difunctionalization of double bonds via an ATRA-type mechanism. *J. Org. Chem.* **81**, 6945–6952 (2016).
5. Reiser, O. Shining light on copper: unique opportunities for visible-light-catalyzed atom transfer radical addition reactions and related processes. *Acc. Chem. Res.* **49**, 1990–1996 (2016).
6. Hossain, A., Bhattacharyya, A. & Reiser, O. Copper's rapid ascent in visible-light photoredox catalysis. *Science* **364**, eaav9713 (2019).
7. Zhong, M., Pannecoucke, X., Jubault, P. & Poisson, T. Recent advances in photocatalyzed reactions using well-defined copper(I) complexes. *Beilstein J. Org. Chem.* **16**, 451–481 (2020).
8. Engl, S. & Reiser, O. Copper-photocatalyzed ATRA reactions: concepts, applications, and opportunities. *Chem. Soc. Rev.* **51**, 5287–5299 (2022).
9. Bagal, D. B. et al. Trifluoromethylchlorosulfonylation of alkenes: evidence for an inner-sphere mechanism by a copper phenanthroline photoredox catalyst. *Angew. Chem. Int. Ed.* **54**, 6999–7002 (2015).
10. Hossain, A., Engl, S., Lutsker, E. & Reiser, O. Visible-light-mediated regioselective chlorosulfonylation of alkenes and alkynes: introducing the Cu(II) complex [Cu(dap)Cl_2] to photochemical ATRA reactions. *ACS Catal.* **9**, 1103–1109 (2019).
11. Bian, K. J., Kao, S. C., Nemoto, D., Chen, X. W. & West, J. G. Photochemical diazidation of alkenes enabled by ligand-to-metal charge transfer and radical ligand transfer. *Nat. Commun.* **13**, 7881 (2022).
12. Bian, K. J. et al. Modular difunctionalization of unactivated alkenes through bio-inspired radical ligand transfer catalysis. *J. Am. Chem. Soc.* **144**, 11810–11821 (2022).
13. Guo, Q. et al. Dual-functional chiral Cu-catalyst-induced photoredox asymmetric cyanofluoroalkylation of alkenes. *ACS Catal.* **9**, 4470–4476 (2019).
14. Lu, B., Cheng, Y., Chen, L. Y., Chen, J. R. & Xiao, W. J. Photoinduced copper-catalyzed radical aminocarbonylation of cycloketone oxime esters. *ACS Catal.* **9**, 8159–8164 (2019).
15. Pirtsch, M., Paria, S., Matsuno, T., Isobe, H. & Reiser, O. Cu(dap)$_2$Cl] as an efficient visible-light-driven photoredox catalyst in carbon–carbon bond-forming reactions. *Chem. Eur. J.* **18**, 7336–7340 (2012).
16. Rawner, T., Lutsker, E., Kaiser, C. A. & Reiser, O. The different faces of photoredox catalysts: visible-light-mediated atom transfer radical addition (ATRA) reactions of perfluoroalkyl iodides with styrenes and phenylacetylenes. *ACS Catal.* **8**, 3950–3956 (2018).
17. Engl, S. & Reiser, O. Copper makes the difference: visible light-mediated atom transfer radical addition reactions of iodoform with olefins. *ACS Catal.* **10**, 9899–9906 (2020).
18. Reichle, A. et al. Copper(I) photocatalyzed bromonitroalkylation of olefins: evidence for highly efficient inner-sphere pathways. *Angew. Chem. Int. Ed.* **62**, e202219086 (2023).
19. Abderazzak, Y. & Reiser, O. Copper photocatalyzed divergent access to organic thio- and isothiocyanates. *ACS Catal.* **14**, 4847–4855 (2024).
20. Groves, J. K. The Friedel–Crafts acylation of alkenes. *Chem. Soc. Rev.* **1**, 73–97 (1972).
21. Miyahara, Y. & Ito, Y. $AlCl_3$-mediated aldol cyclocondensation of 1,6- and 1,7-dions to cyclopentene and cyclohexene derivatives. *J. Org. Chem.* **79**, 6801–6807 (2014).
22. Tanaka, S., Kunisawa, T., Yoshii, Y. & Hattori, T. Acylation of alkenes with the aid of $AlCl_3$ and 2,6-dibromopyridine. *Org. Lett.* **21**, 8509–8513 (2019).
23. Le Roux, C., Gaspard-Iloughmane, H. & Dubac, J. Bismuth(III) halide-catalyzed tandem aldol-halogenation reaction: a convenient synthesis of β-halo ketones and esters. *J. Org. Chem.* **59**, 2238–2240 (1994).
24. Salama, T. A. & Elmorsy, S. S. Silicon mediated synthesis and selected transformations of β-chloroketones. *Chin. Chem. Lett.* **22**, 1171–1174 (2011).

25. Lei, Z. et al. Selective aroylation of activated alkenes by photoredox catalysis. *Angew. Chem. Int. Ed.* **58**, 7318–7323 (2019).
26. Patil, D. V., Kim, H. Y. & Oh, K. Visible light-promoted Friedel–Crafts-type chloroacylation of alkenes to β-chloroketones. *Org. Lett.* **22**, 3018–3022 (2020).
27. Zhou, Y. et al. Photoredox-catalyzed acylchlorination of α-CF_3 alkenes with acyl chloride and application as masked access to β-CF_3-enones. *Org. Lett.* **26**, 2656–2661 (2024).
28. Li, C.-G., Xu, G.-Q. & Xu, P.-F. Synthesis of fused pyran derivatives via visible-light-induced cascade cyclization of 1,7-enynes with acyl chlorides. *Org. Lett.* **19**, 512–515 (2017).
29. Xu, S.-M. et al. Aroyl chlorides as novel acyl radical precursors via visible-light photoredox catalysis. *Org. Chem. Front.* **4**, 1331–1335 (2017).
30. Sarkar, S., Banerjee, A., Yao, W., Patterson, E. V. & Ngai, M.-Y. Photocatalytic radical aroylation of unactivated alkenes: pathway to β-functionalized 1,4-, 1,6-, and 1,7-diketones. *ACS Catal.* **9**, 10358–10364 (2019).
31. Banerjee, A. et al. Excited-state copper catalysis for the synthesis of heterocycles. *Angew. Chem. Int. Ed.* **61**, e202113841 (2022).
32. Sarkar, S., Banerjee, A. & Ngai, M.-Y. Synthesis of ketonylated carbocycles via excited-state copper-catalyzed radical carbo-aroylation of unactivated alkenes. *ChemCatChem* **15**, e202201128 (2023).
33. Zhao, Q.-S., Xu, G.-Q., Liang, H., Wang, Z.-Y. & Xu, P.-F. Aroylchlorination of 1,6-dienes via a photoredox catalytic atom-transfer radical cyclization process. *Org. Lett.* **21**, 8615–8619 (2019).
34. Engl, S. & Reiser, O. Making copper photocatalysis even more robust and economic: photoredox catalysis with $[Cu^{II}(dmp)_2Cl]Cl$. *Eur. J. Org. Chem.* **2020**, 1523–1533 (2020).
35. Palmer, C. E. A. & McMillin, D. R. Singlets, triplets, and exciplexes: complex, temperature-dependent emissions from (2,9-dimethyl-1,10-phenanthroline)bis(triphenylphosphine)copper(1+) and (1,10-phenanthroline)(triphenylphosphine)copper(1+). *Inorg. Chem.* **26**, 3837–3840 (1987).
36. Casadonte, D. J. & McMillin, D. R. Dual emissions from (2,9-dimethyl-1,10-phenanthroline)bis(tertiary phosphine) copper(1+) systems in a rigid glass: influence of the phosphine donor strength. *Inorg. Chem.* **26**, 3950–3952 (1987).
37. Cortes, P. A. F., Marx, M., Trose, M. & Beller, M. Heteroleptic copper complexes with nitrogen and phosphorus ligands in photocatalysis: overview and perspectives. *Chem. Catal.* **1**, 298–338 (2021).
38. Minozzi, C., Caron, A., Grenier-Petel, J.-C., Santandrea, J. & Collins, S. K. Heteroleptic copper(I)-based complexes for photocatalysis: combinatorial assembly, discovery, and optimization. *Angew. Chem. Int. Ed.* **57**, 5477–5481 (2018).
39. Hernandez-Perez, A. C. & Collins, S. K. Heteroleptic Cu-based sensitizers in photoredox catalysis. *Acc. Chem. Res.* **49**, 1557–1565 (2016).
40. Hernandez-Perez, A. C. & Collins, S. K. A visible-light-mediated synthesis of carbazoles. *Angew. Chem. Int. Ed.* **52**, 12696–12700 (2013).
41. Hernandez-Perez, A. C., Vlassova, A. & Collins, S. K. Toward a visible light mediated photocyclization: Cu-based sensitizers for the synthesis of [5]helicene. *Org. Lett.* **14**, 2988–2991 (2012).
42. Wang, C. et al. Visible-light-driven, copper-catalyzed decarboxylative C(sp^3)–H alkylation of glycine and peptides. *Angew. Chem. Int. Ed.* **57**, 15841–15846 (2018).
43. Lyu, X. L., Huang, S. S., Song, H. J., Liu, Y. X. & Wang, Q. M. Visible-light-induced copper-catalyzed decarboxylative coupling of redox-active esters with N-heteroarenes. *Org. Lett.* **21**, 5728–5732 (2019).
44. Wang, C., Yu, Y., Liu, W.-L. & Duan, W.-L. Site-tunable Csp^3–H bonds functionalization by visible-light-induced radical translocation of N-alkoxyphthalimides. *Org. Lett.* **21**, 9147–9152 (2019).
45. Knorn, M., Rawner, T., Czerwieniec, R. & Reiser, O. Copper-(phenanthroline)(bisisonitrile)$^+$-complexes for the visible-light-mediated atom transfer radical addition and allylation reactions. *ACS Catal.* **5**, 5186–5193 (2015).
46. Caron, A., Morin, É. & Collins, S. K. Bifunctional copper-based photocatalyst for reductive pinacol-type couplings. *ACS Catal.* **9**, 9458–9464 (2019).
47. Bao, H. et al. P/N heteroleptic Cu(I)-photosensitizer-catalyzed deoxygenative radical alkylation of aromatic alkynes with alkyl aldehydes using dipropylamine as a traceless linker agent. *ACS Catal.* **10**, 7563–7572 (2020).
48. Roland, G. et al. [2 + 2] Photocycloadditions to form cyclobutanes and bicyclo[2.1.1]hexanes employing copper-based photocatalysis. *ACS Catal.* **14**, 11490–11497 (2024).
49. Pohland, A. E. & Benson, W. R. β-Chlorovinyl ketones. *Chem. Rev.* **66**, 161–197 (1966).
50. Gooßen, L. J., Rodríguez, N. & Gooßen, K. Stereoselective synthesis of β-chlorovinyl ketones and arenes by the catalytic addition of acid chlorides to alkynes. *Angew. Chem. Int. Ed.* **48**, 9592–9594 (2009).
51. Iwai, T., Fujihara, T., Terao, J. & Tsuji, Y. Iridium-catalyzed addition of acid chlorides to terminal alkynes. *J. Am. Chem. Soc.* **131**, 6668–6669 (2009).
52. Iwai, T., Fujihara, T., Terao, J. & Tsuji, Y. Iridium-catalyzed addition of aroyl chlorides and aliphatic acid chlorides to terminal alkynes. *J. Am. Chem. Soc.* **134**, 1268–1274 (2012).
53. Koo, H., Kim, H. Y. & Oh, K. (E)-Selective Friedel–Crafts acylation of alkynes to β-chlorovinyl ketones: defying isomerizations in batch reactions by flow chemistry approaches. *Org. Chem. Front.* **6**, 1868–1872 (2019).
54. Srebnik, M., Ramachandran, P. V. & Brown, H. C. Chiral synthesis via organoboranes. 18. Selective reductions. 43. Diisopinocampheylchloroborane as an excellent chiral reducing reagent for the synthesis of halo alcohols of high enantiomeric purity. A highly enantioselective synthesis of both optical isomers of tomoxetine, fluoxetine, and nisoxetine. *J. Org. Chem.* **53**, 2916–2920 (1988).
55. Maestro, A., Nagy, B. S., Otvos, S. V. & Kappe, C. O. A telescoped continuous flow enantioselective process for accessing intermediates of 1-aryl-1,3-diols as chiral building blocks. *J. Org. Chem.* **88**, 15523–15529 (2023).
56. Bosset, C. et al. Iron-catalyzed synthesis of C2 aryl- and N-heteroaryl-substituted tetrahydropyrans. *J. Org. Chem.* **80**, 12509–12525 (2015).
57. Lee, Y., Shabbir, S., Jeong, Y., Ban, J. & Rhee, H. Formal synthesis of fesoterodine by acid-facilitated aromatic alkylation. *Bull. Korean Chem. Soc.* **36**, 2885–2889 (2015).
58. Khatik, G. L., Sharma, R., Kumar, V., Chouhan, M. & Nair, V. A. Stereoselective synthesis of (S)-dapoxetine: a chiral auxiliary mediated approach. *Tetrahedron Lett.* **54**, 5991–5993 (2013).
59. Xu, C. & Yuan, C. Candida Rugosa lipase-catalyzed kinetic resolution of β-hydroxy-β-arylpropionates and δ-hydroxy -δ-aryl-β-oxo-pentanoates. *Tetrahedron* **61**, 2169–2186 (2005).
60. Goyal, S. et al. Stereoselective alkylation of imines and its application towards the synthesis of β-lactams. *Asian J. Org. Chem.* **5**, 1359–1367 (2016).
61. Kook, C. S., Reed, M. F. & Digenis, G. A. Preparation of [^{18}F] haloperidol. *J. Med. Chem.* **18**, 533–535 (1975).
62. Zhang, X. & MacMillan, D. W. C. Direct aldehyde C–H arylation and alkylation via the combination of nickel, hydrogen atom transfer, and photoredox catalysis. *J. Am. Chem. Soc.* **139**, 11353–11356 (2017).

63. *Price of 4-Chlorobutanal (€350/50 mg @Sigma)* (Merck, accessed 1 October 2024); https://www.sigmaaldrich.com/DE/de/product/enamine/ena638599301?context=bbe
64. Kuninobou, Y. et al. Indium-catalyzed synthesis of keto esters from cyclic 1,3-diketones and alcohols and application to the synthesis of seratrodast. *Chem. Asian J.* **5**, 941–945 (2010).
65. Marion, L. The alkaloids of *Sedum acre* L. *Can. J. Res.* **23B**, 165 (1945).
66. Tufariello, J. J. & Ali, S. A. The stereochemistry of nitrone cycloadditions. d1-allosedamine and d1-sedridine. *Tetrahedron Lett.* **47**, 4647–4650 (1978).
67. Shono, T., Matsumura, Y. & Tsubata, K. Electroorganic chemistry. 46. A new carbon–carbon bond forming reaction at the α-position of amines utilizing anodic oxidation as a key step. *J. Am. Chem. Soc.* **103**, 1172–1176 (1981).
68. Ozawa, N., Nakajima, S., Zaoya, K., Hamaguchi, F. & Nagasaka, T. A facile synthesis of dl-sedamine and d1-allosedamine. *Heterocycles* **32**, 889–894 (1991).
69. Spangenberg, T., Breit, B. & Mann, A. Hydroformylation of homoallylic azides: a rapid approach toward alkaloids. *Org. Lett.* **11**, 261–264 (2009).
70. Park, Y. & Ryu, J.-S. Formal synthesis of (±)-sedamine through gold(I)-catalyzed intramolecular dehydrative amination of sulfamate esters tethered to allylic alcohols. *Tetrahedron Lett.* **71**, 153024 (2021).
71. Beyerman & Enthoven, P. H. Synthesis of α-phenacyl-*N*-methylpiperil)ine ("sedamine-ketone") under pseudophysiological conditions. Recl. Trav. Chim. Pays-Bas **75**, 82–84 (1956).
72. Beyerman, H. C., Eveleens, W. & Muller, Y. M. F. On the synthesis and stereochemistry of sedamine. *Recl. Trav. Chim. Pays-Bas* **75**, 63–75 (1956).
73. Cossy, J., Willis, C., Bellosta, V. & BouzBouz, S. Enantioselective allyltitanations and metathesis reactions. Application to the synthesis of piperidine alkaloids (+)-sedamine and (−)-prosophylline. *J. Org. Chem.* **67**, 1982–1992 (2002).
74. Felpin, F.-X. & Lebreton, J. A highly stereoselective asymmetric synthesis of (−)-lobeline and (−)-sedamine. *J. Org. Chem.* **67**, 9192–9199 (2002).
75. Angoli, M. et al. Remote stereocenter discrimination in the enzymatic resolution of piperidine-2-ethanol. Short enantioselective synthesis of sedamine and allosedamine. *J. Org. Chem.* **68**, 9525–9527 (2003).
76. Josephsohn, N. S., Snapper, M. L. & Hoveyda, A. H. Ag-catalyzed asymmetric mannich reactions of enol ethers with aryl, alkyl, alkenyl, and alkynyl imines. *J. Am. Chem. Soc.* **126**, 3734–3735 (2004).
77. Zheng, G., Dwoskin, L. P. & Crooks, P. A. Indirect trapping of the retroconjugate addition reaction intermediate involved in the epimerization of lobeline: application to the synthesis of (−)-sedamine. *J. Org. Chem.* **69**, 8514–8517 (2004).
78. Yadav, J. S., Reddy, M. S., Rao, P. P. & Prasad, A. R. Stereoselective synthesis of *anti*-1,3-diol units via Prins cyclisation: application to the synthesis of (−)-sedamine. *Tetrahedron Lett.* **47**, 4397–4401 (2006).
79. Fustero, S., Jimenez, D., Moscardo, J., Catalan, S. & del Pozo, C. Enantioselective organocatalytic intramolecular aza-Michael reaction: a concise synthesis of (+)-sedamine, (+)-allosedamine, and (+)-coniine. *Org. Lett.* **9**, 5283–5286 (2007).
80. Reddy, A. A. & Prasad, K. R. Synthesis of β-amino ketones by addition of aryl methyl ketones to sulfinimines: application to the total synthesis of HPA-12, norsedamine, and sedamine. *J. Org. Chem.* **82**, 13488–13499 (2017).
81. He, J., Chen, C., Fu, G. C. & Peters, J. C. Visible-light-induced, copper-catalyzed three-component coupling of alkyl halides, olefins, and trifluoromethylthiolate to generate trifluoromethyl thioethers. *ACS Catal.* **8**, 11741–11748 (2018).
82. Chen, C., Peters, J. C. & Fu, G. C. Photoinduced copper-catalysed asymmetric amidation via ligand cooperativity. *Nature* **596**, 250–256 (2021).
83. Kainz, Q. M. et al. Asymmetric copper-catalyzed C–N cross-couplings induced by visible light. *Science* **351**, 681–684 (2016).
84. Wang, P.-Z., Zhang, B., Xiao, W.-J. & Chen, J.-R. Photocatalysis meets copper catalysis: a new opportunity for asymmetric multicomponent radical cross-coupling reactions. *Acc. Chem. Res.* **57**, 3433–3448 (2024).
85. Mitani, M., Kato, I. & Koyama, K. Photoaddition of alkyl halides to olefins catalyzed by copper(I) complexes. *J. Am. Chem. Soc.* **105**, 6719–6721 (1983).
86. Cruché, C., Neiderer, W. & Collins, S. K. Heteroleptic copper-based complexes for energy-transfer processes: *E* → *Z* isomerization and tandem photocatalytic sequences. *ACS Catal.* **11**, 8829–8836 (2021).
87. Allgäuer, D. S. et al. Quantification and theoretical analysis of the electrophilicities of Michael acceptors. *J. Am. Chem. Soc.* **139**, 13318–13329 (2017).
88. Huffman, L. M. & Stahl, S. S. Carbon–nitrogen bond formation involving well-defined aryl–copper(III) complexes. *J. Am. Chem. Soc.* **130**, 9196–9197 (2008).
89. King, A. E. et al. Copper-catalyzed aerobic oxidative functionalization of an arene C–H bond: evidence for an aryl–copper(III) intermediate. *J. Am. Chem. Soc.* **132**, 12068–12073 (2010).
90. Huffman, L. M. et al. Observation and mechanistic study of facile C–O bond formation between a well-defined aryl–copper(III) complex and oxygen nucleophiles. *Chem. Eur. J.* **17**, 10643–10650 (2011).

Acknowledgements

This work was supported by the Deutsche Forschungsgemeinschaft (DFG, German Research Foundation), TRR 325444632635-A1. We thank S. Stempfhuber and B. Hischa for X-ray analysis, R. Hoheisel for cyclic voltammetry studies, B. Baumann for EPR measurements and M. Dietel for EPR measurements and helpful scientific discussions. We acknowledge J. Rehbein for her suggestions regarding EPR experiments (all University of Regensburg).

Author contributions

Tirtha Mandal, M.G. and O.R. conceived the concept. Tirtha Mandal and M.G. performed the reactions and analysed the products. Tirtha Mandal, M.G., H.P. and Tanumoy Mandal carried out the mechanistic studies. O.R. supervised the experimental work. Tirtha Mandal, M.G. and O.R. wrote the paper. Tirtha Mandal and M.G. contributed equally to this work.

Funding

Open access funding provided by Universität Regensburg.

Competing interests

The authors declare no competing interests.

Additional information

Extended data is available for this paper at https://doi.org/10.1038/s41929-025-01357-y.

Supplementary information The online version contains supplementary material available at https://doi.org/10.1038/s41929-025-01357-y.

Correspondence and requests for materials should be addressed to Oliver Reiser.

Peer review information *Nature Catalysis* thanks Kyungsoo Oh and the other, anonymous, reviewer(s) for their contribution to the peer review of this work.

https://doi.org/10.1038/s41929-025-01357-y

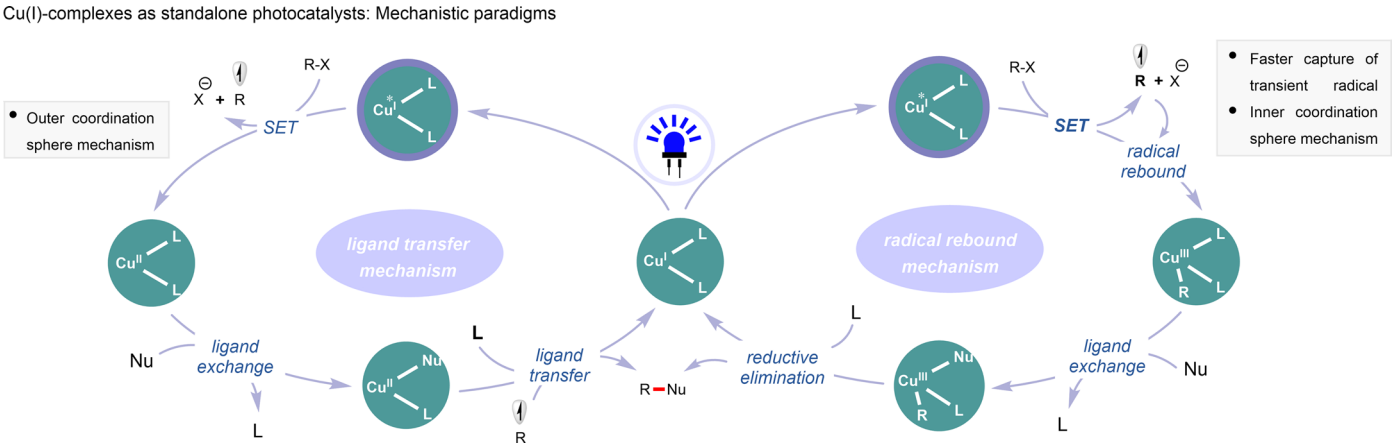

Extended Data Fig. 1 | Cu(I)-Photocatalysis: Mechanistic paradigms. Different facets of Cu(I)-photocatalysis via outer-sphere and inner-sphere electron transfer pathways. Nu = nucleophile, L = ligand.

https://doi.org/10.1038/s41929-025-01357-y

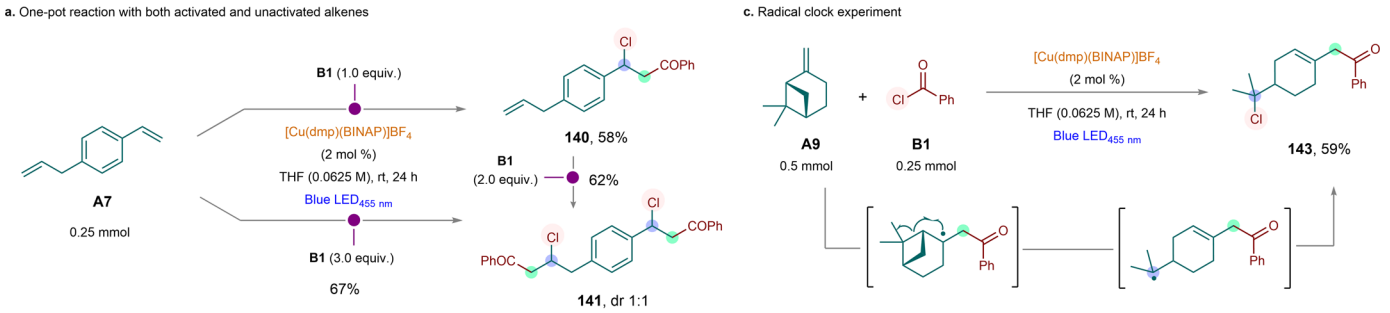

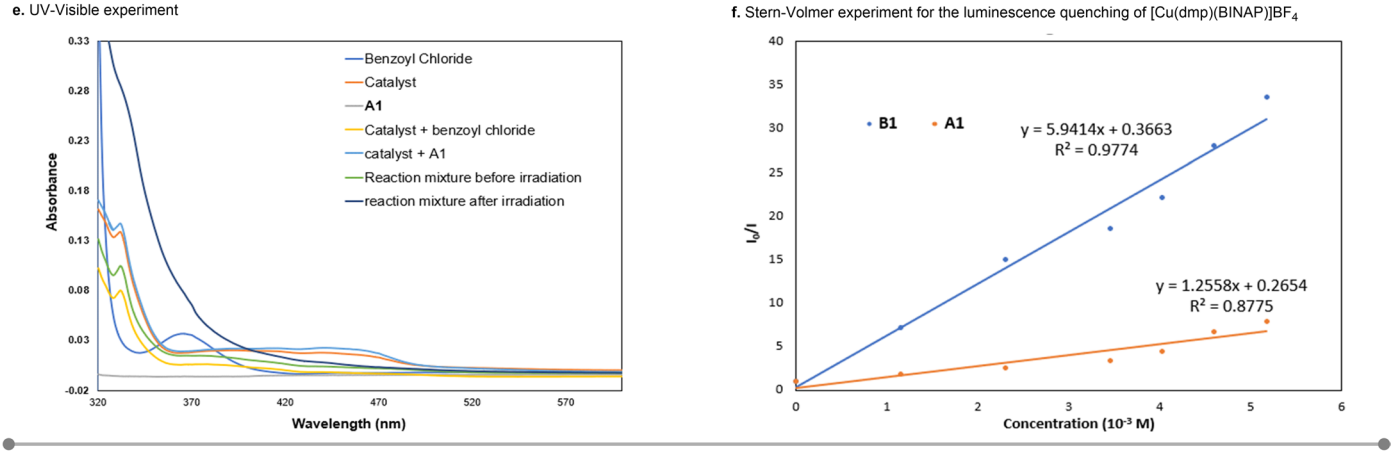

g. Comparative study: Heteroleptic Cu(I)-Photocatalysts

Entry	Photocatalyst	$E_{1/2}(Cu^{II}/Cu^{I*})$ (V vs SCE)	τ^a (ns)	Yield of 1 (%)[b]
1	[Cu(phen)(XantPhos)]BF_4	-1.69	391	Traces
2	[Cu(dmp)(XantPhos)]BF_4	-1.73	1133	12
3	[Cu(phen)(BINAP)]BF_4	-1.60	3.10	30
4	**[Cu(dmp)(BINAP)]BF_4**	**-1.64**	**2188**	**76**
5	[Cu(dmp)(DPEphos)]BF_4	-1.68	14300	10

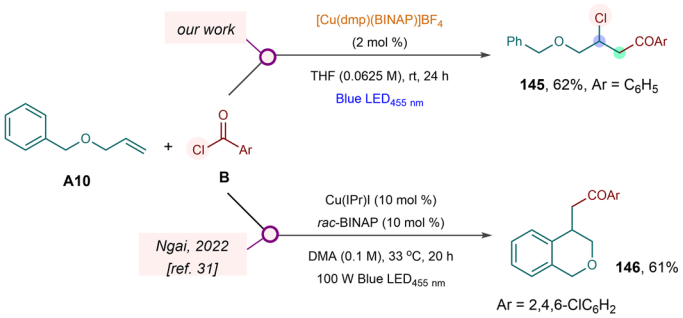

Extended Data Fig. 2 | Mechanistic investigations. Unless otherwise noted yields are of the isolated products. [a]τ = Excited-state lifetime. [b]1H-NMR yields are measured using 1,1,2,2-tetrachloroethane as the internal standard. **a**. β-Chloroacylation in the presence of both activated and unactivated alkenes. **b**. β-Chloroacylation of conjugated diene. **c**. Radical clock experiment with β-pinene. **d**. Radical trapping experiment in the presence of TEMPO. **e**. UV-vis experiment of different reaction components, Cu(I)-catalyst, and reaction mixture before and after irradiation. **f**. Stern-Volmer plot for luminescence quenching of Cu(I)-catalyst in the presence of aroyl chloride and alkene. **g**. Tabular representation of spectroscopic data for different heteroleptic Cu(I)-photocatalysts and their performance in β-Chloroacylation reaction. **h**. β-Chloroacylation vs intramolecular cyclization.